

Short Communication

# Synthesis, Characterization and Electrochemical Properties of a Novel Cobalt-Free $\text{Ba}_{0.5}\text{Sr}_{0.5}\text{Fe}_{0.8}\text{Mn}_{0.2}\text{O}_{3-\alpha}$ Intermediate-Temperature Cathode Material

Zhijie Yang<sup>1</sup>, Huihuang Jiang<sup>2,\*</sup>, Hongtao Wang<sup>3,\*\*</sup>

<sup>1</sup> Suzhou Dingan Technology Co., Ltd., Suzhou 215100, PR China.

<sup>2</sup> School of Art, Soochow University, Suzhou 215123, PR China.

<sup>3</sup> School of Chemical and Material Engineering, Fuyang Normal University, Fuyang 236037, China

\*E-mail: [jianghuihuang@suda.edu.cn](mailto:jianghuihuang@suda.edu.cn), [hwang@fynu.edu.cn](mailto:hwang@fynu.edu.cn)

Received: 26 August 2020 / Accepted: 10 October 2020 / Published: 31 October 2020

In this paper, a novel cobalt-free cathode of  $\text{Ba}_{0.5}\text{Sr}_{0.5}\text{Fe}_{0.8}\text{Mn}_{0.2}\text{O}_{3-\alpha}$  (BSFMn) and electrolyte of  $\text{BaZr}_{0.1}\text{Ce}_{0.7}\text{Y}_{0.2}\text{O}_{3-\alpha}$  (BZCY) were prepared by nitrate citric acid method. A single cell of NiO-BZCY | BZCY | BSFMn was assembled by a simple and effective slurry spin coating method and its  $\text{H}_2/\text{air}$  fuel cell performance was also tested. The BSFMn, BZCY and NiO-BZCY were analyzed by X-ray diffraction (XRD). And a single cell after testing was analyzed using scanning electron microscopy (SEM). The maximum output power densities of NiO-BZCY | BZCY | BSFMn were  $216 \text{ mW}\cdot\text{cm}^{-2}$ ,  $351 \text{ mW}\cdot\text{cm}^{-2}$  and  $500 \text{ mW}\cdot\text{cm}^{-2}$  at  $600^\circ\text{C}$ ,  $650^\circ\text{C}$  and  $700^\circ\text{C}$ , respectively.

**Keywords:** Cathode; Electrolyte; Fuel cell; Anode; Nitrate citric acid method

## 1. INTRODUCTION

A solid oxide fuel cell (SOFC) is an efficient and low pollution device that converts chemical energy into electrical energy [1–6]. SOFCs consist of an anode, electrolyte, cathode and connecting material. As the core component of the fuel cell, the solid electrolyte must meet the requirements of high ionic conductivity, compactness and structural stability [7–12]. In recent years,  $\text{ZrO}_2$  based,  $\text{CeO}_2$  based electrolytes with fluorite structures and  $\text{ABO}_3$  electrolytes with perovskite structures have mainly been used. Among them,  $\text{BaZr}_{0.1}\text{Ce}_{0.7}\text{Y}_{0.2}\text{O}_{3-\alpha}$  perovskite-type oxide has attracted much attention as it reduces the operating temperature of the fuel cell to  $500\text{--}800^\circ\text{C}$  and has excellent properties.

The working condition of the cathode is different from that of the electrolyte, with a high temperature oxidation atmosphere and requiring high electronic conductivity, adequate porosity and

high catalytic activity. At present, the most studied are  $ABO_3$ ,  $AA'B_2O_5$  and  $A_2BO_4$  type cathodes. Cobalt-containing cathode materials such as  $Ba_{1-x}Co_{0.7}Fe_{0.2}Ni_{0.1}O_{3-\alpha}$ , and  $Ba_xSr_{1-x}Co_{0.8}Nb_{0.2}O_{3-\alpha}$  have excellent electrochemical performance and high electrocatalytic activity [13–15]. However, these cobalt-containing cathodes have poor chemical stability, easily volatilize at high temperature, have a mismatched coefficient of thermal expansion and are expensive, etc. In order to overcome the problems brought about by these shortcomings, many researches have turned to cobalt-free cathode materials [16–20].

In this paper,  $Ba_{0.5}Sr_{0.5}Fe_{0.8}Mn_{0.2}O_{3-\alpha}$  (BSFMn) and  $BaZr_{0.1}Ce_{0.7}Y_{0.2}O_{3-\alpha}$  (BZCY) were prepared by the nitrate citric acid method. The anode supported BZCY electrolyte semi-cell was prepared by a simple and effective slurry spin coating method. A single cell of NiO-BZCY | BZCY | BSFMn was assembled and its  $H_2$ /air fuel cell performance was tested.

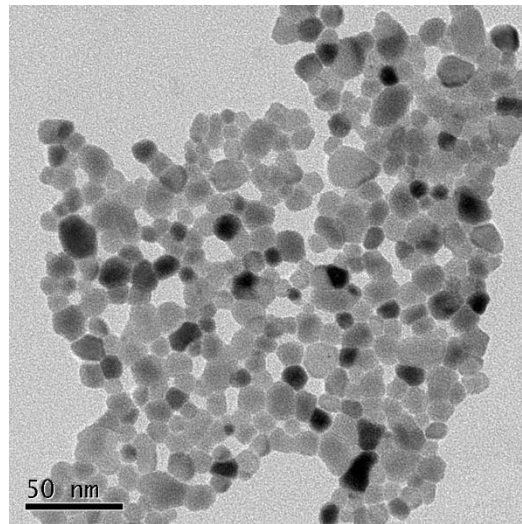
## 2. EXPERIMENTAL

Cobalt-free cathode material,  $Ba_{0.5}Sr_{0.5}Fe_{0.8}Mn_{0.2}O_{3-\alpha}$  (BSFMn), was prepared by the nitrate citric acid method. Stoichiometric raw materials of  $Ba(NO_3)_2$ ,  $Sr(NO_3)_2$ ,  $Fe(NO_3)_3 \cdot 9H_2O$  and  $Mn(NO_3)_2 \cdot 4H_2O$  were dissolved in deionized water to form a nitrate solution of metal salts. Citric acid was added as a complexing agent. The ratio of total metal cations and citric acid was 1:2. The above solution was placed at 90 °C until a dry gel. After heating, the dried gel was ignited to black fluffy precursor powder, then calcined at 600 °C and 1000 °C for 2 h and 5 h, respectively, to obtain BSFMn. Electrolyte of  $BaZr_{0.1}Ce_{0.7}Y_{0.2}O_{3-\alpha}$  (BZCY) was prepared by the same method. After being calcined at 1100 °C for 10 h, BZCY was obtained.

The BZCY powder prepared above was mixed with nickel oxide, and a certain amount of activated carbon and starch were added as a pore forming agent. The weight ratio was BZCY : NiO : activated carbon : starch = 35 : 65 : 5 : 5. After being pressed and calcined at 1000 °C for 2 h, the anode support of NiO-BZCY was obtained. The prepared electrolyte slurry of BZCY was covered on the polished anode support by a spin coating method. After calcination at 1400 °C for 5 h, a semi-cell of NiO-BZCY | BZCY was prepared. Finally, the prepared cathode slurry of BSFMn was coated on the semi-cell and burned at 950 °C for 2 h to obtain a sandwich type fuel cell: NiO-BZCY | BZCY | BSFMn.

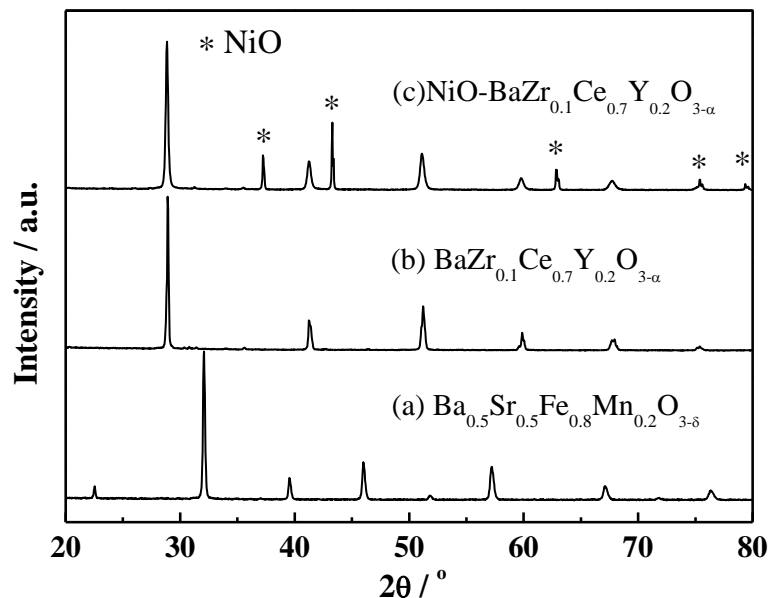
The precursor powder of the cathode material was analyzed by transmission electron microscopy (TEM). The  $Ba_{0.5}Sr_{0.5}Fe_{0.8}Mn_{0.2}O_{3-\alpha}$  (BSFMn),  $BaZr_{0.1}Ce_{0.7}Y_{0.2}O_{3-\alpha}$  (BZCY) and NiO-BZCY were analyzed by X-ray diffraction (XRD). SEM photos of sintered  $Ba_{0.5}Sr_{0.5}Fe_{0.8}Mn_{0.2}O_{3-\alpha}$  (BSFMn),  $BaZr_{0.1}Ce_{0.7}Y_{0.2}O_{3-\alpha}$  (BZCY) and single cell after testing were analyzed. The electrode surfaces of single cell were coated with 0.5 cm<sup>2</sup> silver-palladium paste and sealed at 900 °C for 0.5 h. Air was introduced into the cathode chamber as an oxidant and hydrogen was introduced into the anode. The AC impedance spectra and performances of the fuel cell at 600 °C, 650 °C and 700 °C were tested.

### 3. RESULTS AND DISCUSSION



**Figure 1.** TEM photo of the precursor powder of BSFMn.

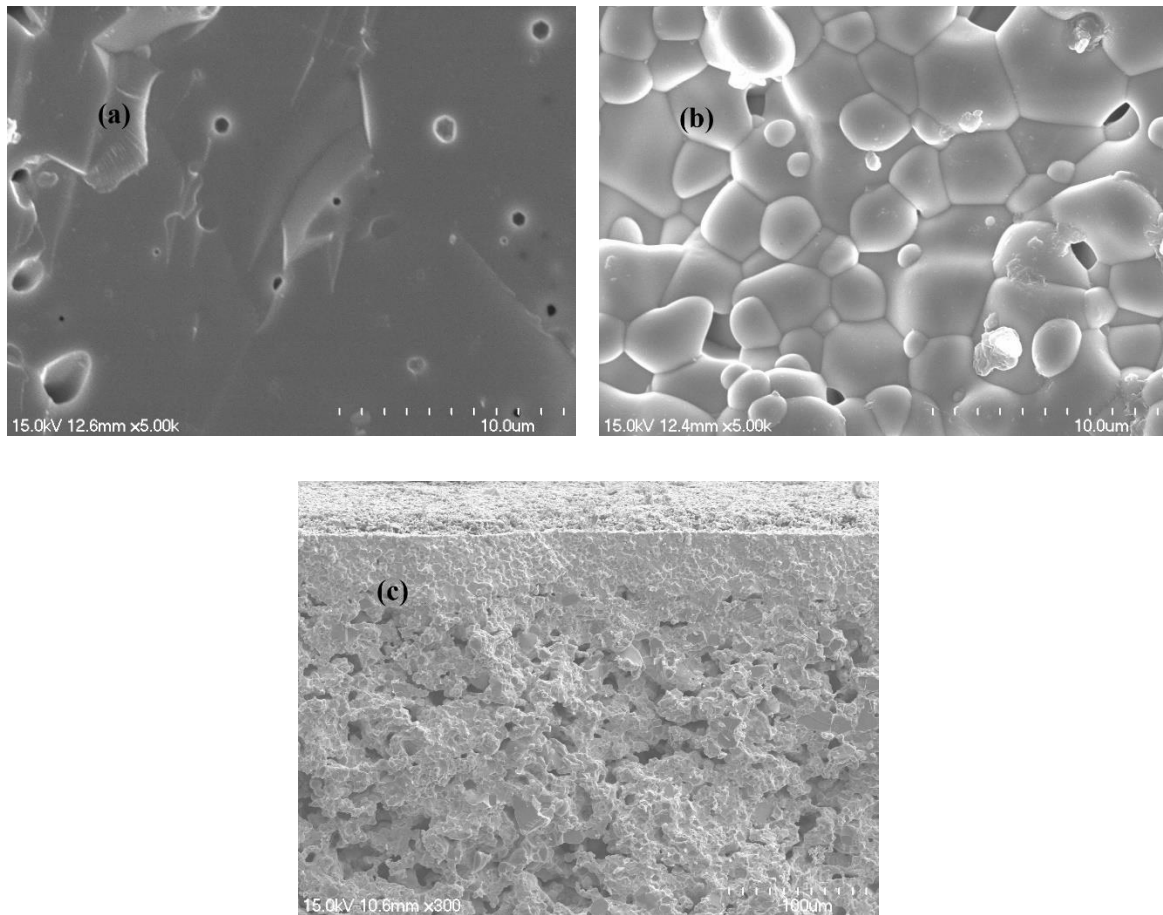
Fig.1 is a TEM photo of the precursor powder of BSFMn prepared by the nitrate citric acid method. Metal ions and citric acid complex well. The powder has uniform particle size of about ten nanometers, and there is no obvious agglomeration phenomenon.



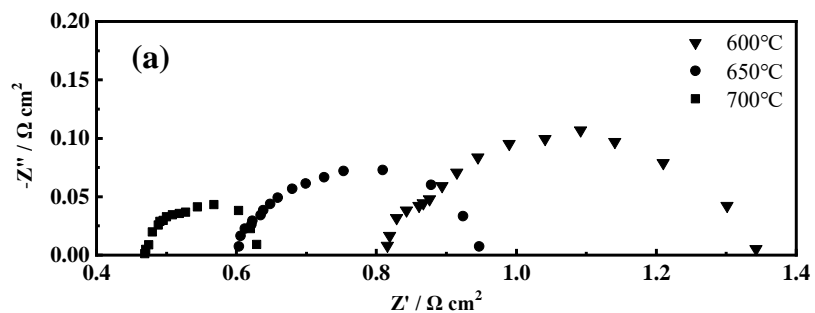
**Figure 2.** XRD patterns of (a)  $\text{Ba}_{0.5}\text{Sr}_{0.5}\text{Fe}_{0.8}\text{Mn}_{0.2}\text{O}_{3-\alpha}$  (BSFMn), (b)  $\text{BaZr}_{0.1}\text{Ce}_{0.7}\text{Y}_{0.2}\text{O}_{3-\alpha}$  (BZCY) and (c) NiO-BZCY.

X-ray diffraction patterns of  $\text{Ba}_{0.5}\text{Sr}_{0.5}\text{Fe}_{0.8}\text{Mn}_{0.2}\text{O}_{3-\alpha}$  (BSFMn),  $\text{BaZr}_{0.1}\text{Ce}_{0.7}\text{Y}_{0.2}\text{O}_{3-\alpha}$  (BZCY) and NiO-BZCY were analyzed and are shown in Fig. 2. It can be seen that the single perovskite structure of BSFMn is formed after sintering at 1000 °C for 5 h. The single perovskite structure of

BZCY is also obtained after the electrolyte film was sintered at 1400 °C for 5 h. Fig. 2(c) is the XRD pattern of anode support, where the symbol \* indicates the diffraction peaks of nickel oxide. No other new peak is found in the anode support, indicating that NiO and BZCY have good chemical compatibility and no new material is produced [21].



**Figure 3.** SEM photos of sintered (a)  $\text{Ba}_{0.5}\text{Sr}_{0.5}\text{Fe}_{0.8}\text{Mn}_{0.2}\text{O}_{3-\alpha}$  (BSFMn), (b)  $\text{BaZr}_{0.1}\text{Ce}_{0.7}\text{Y}_{0.2}\text{O}_{3-\alpha}$  (BZCY) and (c) single cell after tested.



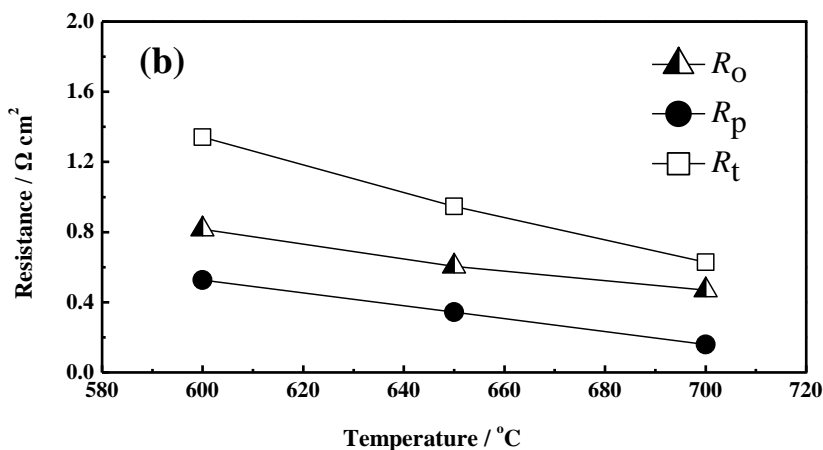


**Figure 4** (a) AC impedance spectra of single cell (NiO-BZCY | BZCY | BSFMn) at 600 °C, 650 °C and 700 °C. (b) relationship between polarization impedance ( $R_p$ ), electrolyte impedance ( $R_o$ ) and total impedance ( $R_t$ ) with temperature under open circuit condition.

SEM photos of sintered  $\text{Ba}_{0.5}\text{Sr}_{0.5}\text{Fe}_{0.8}\text{Mn}_{0.2}\text{O}_{3-\alpha}$  (BSFMn),  $\text{BaZr}_{0.1}\text{Ce}_{0.7}\text{Y}_{0.2}\text{O}_{3-\alpha}$  (BZCY) and single cell after testing are shown in Fig. 3. Fig. 3(a) is the SEM photo of the cross-section of BSFMn after being sintered at 1000 °C for 5 h. The BSFMn has good compactness with only a few small pits and no through holes. Fig. 3(b) is the SEM photo of the electrolyte film surface. It is obvious that the BZCY film is dense and flat with a few pits. The grain growth is good and the diameter is about 3-5  $\mu\text{m}$ . Fig. 3(c) shows the cross-section photo after single cell test. The thickness of the BZCY film is about 40  $\mu\text{m}$ . the electrolyte section is dense and uniform and it is closely combined with the electrode. Both the anode support and cathode are porous, which greatly increases the interface phase reaction [22–23].

Polarization impedance is one of the important factors for the excellent performance of fuel cells. In order to evaluate the performance of BSFMn in a solid oxide fuel cell (SOFC), AC impedance spectra of single cell (NiO-BZCY | BZCY | BSFMn) at 600 °C, 650 °C and 700 °C under an open circuit condition were tested and are shown in Fig. 4. In Fig. 4(a), the intercept of the low frequency part on the real axis is generally considered as the total resistance ( $R_t$ ), while the high frequency part on the real axis represents the electrolyte impedance ( $R_o$ ). The difference between the two represents the polarization impedance ( $R_p$ ). In Fig. 4(b), the electrolyte impedances ( $R_o$ ) are 0.816  $\Omega \cdot \text{cm}^2$ , 0.604  $\Omega \cdot \text{cm}^2$  and 0.469  $\Omega \cdot \text{cm}^2$  at 600 °C, 650 °C and 700 °C, respectively. The polarization impedances ( $R_p$ ) are 0.526  $\Omega \cdot \text{cm}^2$ , 0.343  $\Omega \cdot \text{cm}^2$  and 0.16  $\Omega \cdot \text{cm}^2$ , correspondingly. Our results are less than those of Ding et al., which polarization impedance of NiO-BZCY | BZCY |  $\text{Nd}_{0.7}\text{Sr}_{0.3}\text{MnO}_{3-\alpha}$  single cell were 0.72  $\Omega \cdot \text{cm}^2$ , 0.5  $\Omega \cdot \text{cm}^2$  and 0.17  $\Omega \cdot \text{cm}^2$  at 600 °C, 650 °C and 700 °C, respectively [22].

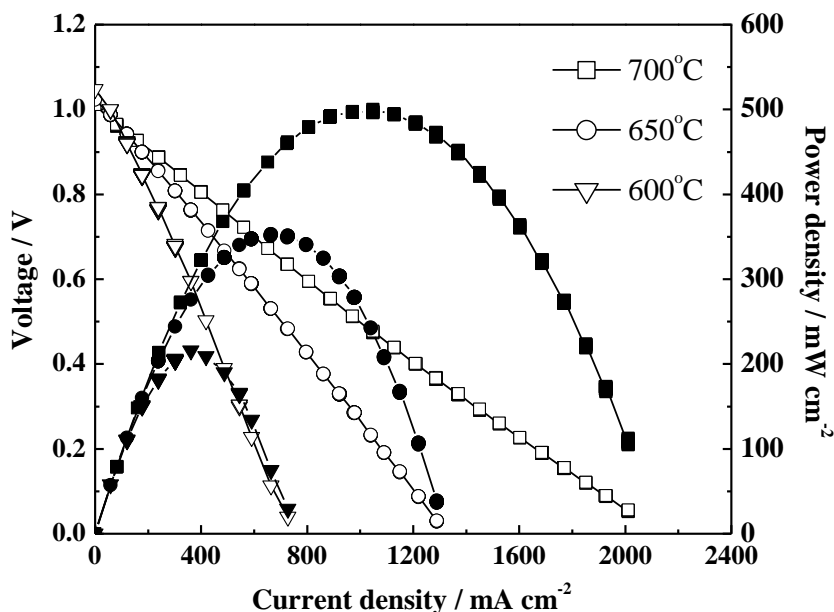


**Figure 5.** *I-V* and *I-P* curves of NiO-BZCY | BZCY | BSFMn at 600 °C, 650 °C and 700 °C.

Figure 5 shows the *I-V* and *I-P* curves of NiO-BZCY | BZCY | BSFMn at 600 °C, 650 °C and 700 °C. The open circuit voltages are 1.048 V, 1.023 V and 1.011 V, respectively, which are close to the theoretical values, indicating that the BZCY electrolyte film is very dense. The *I-V* curves are linear with the increase of current densities, which indicates that there is almost no electrode polarization phenomenon. The maximum output power densities are 216 mW·cm<sup>-2</sup>, 351 mW·cm<sup>-2</sup> and 500 mW·cm<sup>-2</sup> at 600 °C, 650 °C and 700 °C, respectively.

#### 4. CONCLUSIONS

In this paper, a single cell of NiO-BZCY | BZCY | BSFMn was assembled by a simple and effective slurry spin coating method. The XRD patterns indicated that BSFMn and BZCY obtained single perovskite structures after being sintered at 1000 °C and 1400 °C for 5 h, respectively. The SEM photo of the BZCY film shows it is dense and the thickness is about 40 μm. The polarization impedance ( $R_p$ ) of single cell under an open circuit condition were 0.526 Ω·cm<sup>2</sup>, 0.343 Ω·cm<sup>2</sup> and 0.16 Ω·cm<sup>2</sup> at 600 °C, 650 °C and 700 °C, correspondingly. The maximum output power densities of NiO-BZCY | BZCY | BSFMn were 216 mW·cm<sup>-2</sup>, 351 mW·cm<sup>-2</sup> and 500 mW·cm<sup>-2</sup> at 600 °C, 650 °C and 700 °C, respectively.

#### References

1. G. L. Liu, W. Liu, Q. Kou and S. J. Xiao, *Int. J. Electrochem. Sci.*, 13 (2018) 2641.
2. L. Bi, S.P. Shafi, E.H. Da'as and E. Traversa, *Small*, 14 (2018) 1801231.
3. Y. Tian, Z. Lü, X. Guo and P. Wu, *Int. J. Electrochem. Sci.*, 14 (2019) 1093.

4. L. Sun, H. Wang, L. Sheng and H. Li, *Int. J. Electrochem. Sci.*, 12 (2017) 9689.
5. Y.P. Xia, Z.Z. Jin, H.Q. Wang, Z. Gong, H.L. Lv, R.R. Peng, W. Liu and L. Bi, *J. Mater. Chem. A*, 7 (2019) 16136.
6. X. Xu, L. Bi and X.S. Zhao, *J. Membrane Sci.*, 558 (2018) 17.
7. X. Xu, H.Q. Wang, J.M. Ma, W.Y. Liu, X.F. Wang, M. Fronzi and L. Bi, *J. Mater. Chem. A*, 7 (2019) 18792.
8. Y. N. Chen, T. Tian, Z. H. Wan, F. Wu, J. T. Tan and M. Pan, *Int. J. Electrochem. Sci.*, 13 (2018) 3827.
9. A.A. Solovyev, S.V. Rabotkin, A.V. Shipilova and I.V. Ionov, *Int. J. Electrochem. Sci.*, 14 (2019) 575.
10. J.M. Ma, Z.T. Tao, H.N. Kou, M. Fronzi and L. Bi, *Ceram. Int.*, 46 (2020) 4000.
11. H. Ding and X. Xue, *J. Power Sources*, 195(2010) 4139.
12. H. Dai, H. Kou, Z. Tao, K. Liu, M. Xue, Q. Zhang, L. Bi, *Ceram. Int.*, 46 (2020) 6987.
13. N. Sakai, H. Kishimoto, K. Yamaji, T. Horita, M.E. Brito and H. Yokokawa, *J. Electrochem. Soc.*, 154 (2007) B1331.
14. S. Li, Z. Lü, B. Wei, X. Huang, J. Miao, G. Cao, R. Zhu and W. Su, *J. Alloys Compd.*, 426 (2006) 408.
15. K. Wang, R. Ran, W. Zhou, H. Gu, Z. Shao and J. Ahn, *J. Power Sources*, 179 (2008) 60.
16. B. Wei, Z. Lu, X.Q. Huang, M.L. Liu, N. Li, and W.H. Su, *J. Power Sources*, 176 (2008) 1.
17. L. Zhao, B. He, X.Z. Zhang, R.R. Peng, G.Y. Meng and X.Q. Liu, *J. Power Sources*, 195 (2010) 1859.
18. Z.P. Shao and S.M. Haile, *Nature*, 431 (2004) 170.
19. A. Tarancón, D. Marrero-López, J. Peña-Martínez, J.C. Ruiz-Morales and P. Núñez, *Solid State Ionics*, 179 (2008) 611.
20. E. Bucher, A. Egger, G.B. Caraman and W. Sitte, *J. Electrochem. Soc.*, 155 (2008) B1218.
21. I-M. Hung, C.-J. Ciou, Y.-J. Zeng, J.-S. Wu, Y.-C. Lee, A. Su, S.-H. Chan, *J. Eur. Ceram. Soc.*, 31 (2011) 3095.
22. X. Ding, J. Gu, D. Gao, G. Chen, Y. Zhang, *J. Power Sources*, 195 (2010) 4252.
23. K. Chen, Y. Tian, Z. Lü, N. Ai, X. Huang, W. Su, *J. Power Sources*, 186 (2009) 128.